IEEE Access
Multidisciplinary | Rapid Review | Open Access Journal

Received August 19, 2018, accepted September 16, 2018, date of publication October 17, 2018, date of current version November 9, 2018.

Digital Object Identifier 10.1109/ACCESS.2018.2876545

Iterative Learning Control Based Robust Distributed Algorithm for Non-Holonomic Mobile Robots Formation

SHIHAO SUN[1], TAKAHIRO ENDO[2], AND FUMITOSHI MATSUNO[2]
[1]School of Automation Science and Electrical Engineering, Beihang University, Beijing 100191, China
[2]Department of Mechanical Engineering and Science, Kyoto University, Kyoto 606-8501, Japan

Corresponding author: Shihao Sun (jxcrssh@126.com)

This work was supported in part by the NSFC under Grant 61520106010, Grant 61521091, and Grant 61327807, and in part by the National Basic Research Program of China (973 Program) under Grant 2012CB821200 and Grant 2012CB821201.

ABSTRACT This paper presents an iterative learning control-based robust distributed algorithm on the formation issue for a group of differential-drive mobile robots. The fundamental robustness problem in practical application involving initial state shifts, disturbances, noises, and communication time-delays are considered. The distributed algorithm is proposed for each robot in directed network, which is based on the iterative learning rule with both predictive and current learning terms. It is shown that the convergence of formation tracking objective can be guaranteed under a matrix norm condition by using the two-dimensional analysis approach. Numerical simulation and experiment are both given to validate the effectiveness of the proposed algorithm.

INDEX TERMS Iterative learning control, differential-drive mobile robots, robust formation control.

I. INTRODUCTION

Formation control is one of the most challenging problems in the collaboration of multiple mobile robots, which has attracted significant attention in the robot research community over the past decades [1]–[3]. In general, the mobile robots formation can be described as controlling a group of mobile robots track a desired trajectory while maintaining a desired geometric shape including positions and orientations. Using such certain shape, the multiple mobile robots system can accomplish many complex tasks such as environment reconnaissance [5], pursue and capture a group of evaders [6], and transportation of large objects [4].

Apart from high level planning, the trajectory tracking control is the key issue in the formation task, and many works have been carried out on designing formation control strategies for multiple robots system. For example, [7] proposed a three-level hybrid control architecture for controlling multiple mobile robots to achieve formation based on a leader-following approach; [8] studied the execution of different formation-control missions by using the null-space-based behavioral control strategy. However, the communication delays, noise and disturbance are not considered in [7] and [8]. It is common to observe from the numerical experiments that the communication delays among robots occur frequently due to the limited information transmission speed. Moreover, the noise and disturbance are inevitable for a mobile robot moving in the real environment. Therefore, investigating the effect of the communication delays, noise and disturbance in formation control problem is an interesting and important research topic. A pioneering result about robust control with decoupling performance is first obtained in [9] for mobile vehicle by proposing a novel reduction method for nonlinear system model, base on which better maneuverability can be achieved compared with the traditional triangle decoupling control. Reference [10] proposed an improved receding horizon controller to solve the leader-follower formation problem for multi-robot systems with bounded time-varying communication delays and asynchronous clock. The stability analysis and the consensus protocol for the multi-agent system with time-varying delay have been investigated in [11]. The robust formation problem for a multi-robots system affected by measurements noise, disturbance or un-modeled perturbations has been addressed by several authors [12]–[15]. Especially, in [15] a new predictive approach is first proposed to reduce the conservativeness for the analysis and design of uncertain continuous-time systems, by which a group of existing results can be easily derived. Furthermore, [16]–[20] investigated

the consensus of multi-agent systems with communication delays under disturbance and noisy environments. However, the proposed algorithms in the above references can not solve the formation control for multiple non-holonomic mobile robots under the realistic situation involving initial state shifts, disturbances, noises, and communication time-delays simultaneously.

Iterative learning control (ILC) technique is a well established control strategy, which utilizes the information obtained from the previous trial as experience to improve the control performance for the current trial, and many significant theory results have been established and have been widely applied to deal with many practical applications [21]–[29]. Therefore, under the circumstances that the cooperative multiple mobile robots working on repetitive tasks over finite-time interval, such as building-cleaning, parts-transporting, storage, security and patrol, and the ILC is a preferable approach to improve the trajectory tracking performance. Actually, many promising attempts have been considered to improve the control performance for multi-agent systems formation by using ILC. For example, [30] employed the ILC scheme to generate a sequence of control signals for multi-agent formation control problem, but the fixed communication topology without any time-delay and the multi-agent system without any measurement noise and disturbance are the assumed conditions in [30]. In [31], the result obtained in [30] is expanded to formation description independent of the interaction by introducing a ''virtual leader''. In [32], the robust control problem is considered against the uncertainties using the two-dimensional (2-D) analysis approach for ILC. However, the convergence results in [30]–[32] are obtained by the assumptions that the number of system outputs is greater than the number of system inputs and the matrix $C(k+1)B(k)$ has full-row rank, which are not satisfied for differential-drive mobile robots with nonholonomic constraints. In order to release these assumptions, there are two ways, one is to transform the kinematic model of differential-drive mobile robot from the non-holonomic to the holonomic by defining a hand position P (placed at a fixed distance $d > 0$ on the robot) as the control point instead of the center of robot, as in [33] and [34]. However, the orientation of the mobile robot cannot be controlled under this transformation. The other is to assume that there exits a unique control signal for the mobile robot exactly tracks the desired trajectory, which can be achieved by planning a trajectory satisfied the non-holonomic constraint, as stated in [35]–[37]. But the ideal situation without disturbances and noises are considered in there. So far, to the best of our knowledge, for the problem of employing ILC scheme to solve the non-holomonic mobile robot formation problem under a general and realistic condition, there are no such results in the existing literature, which motivates our present study.

In view of the ILC scheme can achieve high-performance tracking, in this paper, we attempt to present a distributed ILC algorithm for a group of non-holonomic mobile robots to form a desired geometric formation shape in the realistic situation involving the initial state shifts, disturbances, noises, and communication time-delays. The reference trajectory for the robots system is represent by a virtual leader and the output of this virtual robot is accessible by only a subset of the real robots according to the directed and fixed communication topology. The iterative learning rule makes use of both predictive and current learning terms to help the tracking errors to converge more quickly than only use predictive learning term. Furthermore, using measurement time-labeled technique as in [10], the accurate delay is calculated to compensate the delay effect in current learning term. With the help of the 2-D analysis approach and graph theory, it is shown that the convergence of the robots system can be robustly ensured under the proposed distributed iterative learning controller. Finally, the simulation and experiment tests are performed to prove that the desired formation task can be effectively and robustly accomplished by using the proposed distributed algorithm. By comparison with the existing results, the main contributions of this paper lie in three aspects:

1) We extend the results in [30]–[32] and [38] about developing the ILC-motivated distributed algorithm for the multi-agent system imposed constraint on the number of system inputs and outputs, which is not satisfied by the non-holomonic mobile robot system.

2) Comparing with the result in [35], which proposes a high-order internal model based ILC scheme for three differential-drive mobile robots formation, the distributed ILC-based algorithm developed in this paper has a uniform controller form for each robot and can easy expand to a general formation problem.

3) Comparing with the results in [8], [10], and [12]–[14], the fundamentally problem in practice involving the initial state shifts, disturbances, noises, and communication time-delays are considered, and a experiment using real differential-drive mobile robots is conducted, which is critical in illustrating the effectiveness of the algorithm for practical application.

The rest of this paper is organized as follows. Problem formulation of differential-drive mobile robots formation is given in Section II. The distributed iterative learning algorithm is constructed in Section III and the convergence of the multi-robot system formation error is analyzed. Comparative simulation results and verifying experimental results are shown in Section IV. Finally, we conclude this paper in Section VI.

Notation 1: $\mathbb{Z}_+ = \{0, 1, \cdots, N\}$, $\mathcal{I}_n = \{1, 2, \cdots, n\}$, I_n denotes the $n \times n$ dimensions identity matrix, $O_{m\times n}$ denotes the $m \times n$ dimensions null matrix, and a diagonal matrix, whose off-diagonal (block) elements are zero and diagonal elements are given by $\{D_1, D_2, \cdots, D_n\}$, is denoted as $diag\{D_1, D_2, \cdots, D_n\}$. $\|A\|$ denotes the norm of a vector (or, matrix) A and $A \geq 0$ means elements in A are all nonnegative. $A \otimes B$ denotes the Kronecker product.

II. PROBLEM DESCRIPTION

A. COMMUNICATION TOPOLOGY AMONG THE MULTI-ROBOT SYSTEMS

In this paper, we assume that the multi-robot system consists of n differential-drive mobile robots labeled 1 through n, and each robot is a vertex in a nth order directed graph $\mathcal{G}$. Denote the vertex set, edge set and weighted adjacency matrix of $\mathcal{G}$ as $\mathcal{V}(\mathcal{G}) = \{v_i : i \in \mathcal{I}_n\}$, $\mathcal{E} \subseteq \{(v_i, v_j) : v_i, v_j \in \mathcal{V}(\mathcal{G})\}$, $\mathcal{A} = [a_{ij}]$, respectively and the v_i's neighbor set is defined as $\mathcal{N}_i = \{j : (v_i, v_j) \in \mathcal{E}(\mathcal{G})\}$. Then the Laplacian matrix of $\mathcal{G}$ can be denoted by $\mathcal{L}_{\mathcal{A}} = \Delta_{\mathcal{A}} - \mathcal{A}$, where $\Delta_{\mathcal{A}}$ is the diagonal matrix: $\Delta_{\mathcal{A}} = diag\left\{\sum_{j\in\mathcal{N}_1} a_{1j}, \sum_{j\in\mathcal{N}_2} a_{2j}, \ldots, \sum_{j\in\mathcal{N}_n} a_{nj}\right\}$, and the edge (v_i, v_j) in $\mathcal{E}(\mathcal{G})$ can be regarded as the available channel, where information flows from the robot v_j to the robot v_i. Moreover, we assume that there exist a virtual robot v_0 in the multi-robot system, which generates a reference trajectory for only a portion of the robots, and each mobile robot in the directed graph network should keep a desired deviation from this reference trajectory. The directed graph $\mathcal{G}$ incorporating virtual robot v_0 is denote as $\tilde{\mathcal{G}}$ and the accessibility of virtual robot v_0 by the robot v_i is denote as a non-negative weight a_{i0} (i.e. the virtual robot v_0 can be accessed by v_i in $\tilde{\mathcal{G}}$ if and only if $a_{i0} > 0$). The weighted matrix associated with the accessibility of reference trajectory for the robots in $\mathcal{G}$ is denote by $\Omega = diag\{a_{10}, a_{20}, \ldots, a_{n0}\}$. Furthermore, for the repetitive formation task, the reference and the deviation are fixed at all iterations over $k \in \mathbb{Z}_+$.

B. MATHEMATICAL MODEL OF THE NONHOLONOMIC MOBILE ROBOT

For $i \in \mathcal{I}_n$, the kinematic motion of the ith differential-drive mobile robot at the kth iteration is given by the following state-space form:

$$\begin{cases} x_{i,k}(t+1) = x_{i,k}(t) + \Delta T \cos\theta_{i,k}(t)[v_{i,k}(t) + Dv_{i,k}(t)] \\ y_{i,k}(t+1) = y_{i,k}(t) + \Delta T \sin\theta_{i,k}(t)[v_{i,k}(t) + Dv_{i,k}(t)] \\ \theta_{i,k}(t+1) = \theta_{i,k}(t) + \Delta T[\omega_{i,k}(t) + D\omega_{i,k}(t)] \\ Yx_{i,k}(t) = x_{i,k}(t) + Nx_{i,k}(t) \\ Yy_{i,k}(t) = y_{i,k}(t) + Ny_{i,k}(t) \\ Y\theta_{i,k}(t) = \theta_{i,k}(t) + N\theta_{i,k}(t) \\ x_{i,k}(0) = x_{i,k0}, y_{i,k}(0) = y_{i,k0}, \theta_{i,k}(0) = \theta_{i,k0} \end{cases} \tag{1}$$

where ΔT is the sampling time, $x_{i,k}(t), y_{i,k}(t), \theta_{i,k}(t)$ are the states of mobile robot which represent the Cartesian coordinates and heading direction in the world frame respectively, $v_{i,k}(t), \omega_{i,k}(t)$ are the control inputs which represent the linear and angular velocities respectively, $Yx_{i,k}(t), Yy_{i,k}(t), Y\theta_{i,k}(t)$ are the system outputs, and $Dv_{i,k}(t), D\omega_{i,k}(t), Nx_{i,k}(t), Ny_{i,k}(t), N\theta_{i,k}(t)$ are the disturbances and measurement noises.

From the above kinematic equation (1), the nonholonomic constraint of the differential-drive mobile robot that the wheel cannot slip in the lateral direction is given in the form as

$$\frac{x_{i,k}(t+1) - x_{i,k}(t)}{\Delta T}\sin\theta_{i,k}(t) - \frac{y_{i,k}(t+1) - y_{i,k}(t)}{\Delta T}\cos\theta_{i,k}(t) = 0 \tag{2}$$

Let

$$\begin{aligned} \xi_{i,k}(t) &= \begin{bmatrix} x_{i,k}(t) & y_{i,k}(t) & \theta_{i,k}(t) \end{bmatrix}^{\mathrm{T}} \\ u_{i,k}(t) &= \begin{bmatrix} v_{i,k}(t) & \omega_{i,k}(t) \end{bmatrix}^{\mathrm{T}} \eta_{i,k}(t) \\ &= \begin{bmatrix} Yx_{i,k}(t) & Yy_{i,k}(t) & Y\theta_{i,k}(t) \end{bmatrix}^{\mathrm{T}} \\ \varsigma_{i,k}(t) &= \begin{bmatrix} Dv_{i,k}(t) & D\omega_{i,k}(t) \end{bmatrix}^{\mathrm{T}} \gamma_{i,k}(t) \\ &= \begin{bmatrix} Nx_{i,k}(t) & Ny_{i,k}(t) & N\theta_{i,k}(t) \end{bmatrix}^{\mathrm{T}} \\ B[\xi_{i,k}(t)] &= \Delta T \begin{bmatrix} \cos\theta_{i,k}(t) & 0 \\ \sin\theta_{i,k}(t) & 0 \\ 0 & 1 \end{bmatrix}, \quad C = \begin{bmatrix} 1 & 0 & 0 \\ 0 & 1 & 0 \\ 0 & 0 & 1 \end{bmatrix} \end{aligned}$$

Then (1) can be rewirrten as

$$\begin{cases} \xi_{i,k}(t+1) = \xi_{i,k}(t) + B[\xi_{i,k}(t)]u_{i,k}(t) \\ \qquad\qquad + B[\xi_{i,k}(t)]\varsigma_{i,k}(t) \\ \eta_{i,k}(t) = C\xi_{i,k}(t) + \gamma_{i,k}(t), \xi_{i,k}(0) = \xi_{i,k0} \end{cases} \tag{3}$$

We first note that the robot motion equation (3) satisfies the following properties.

Property 1: The matrix function $B[\xi_{i,k}(t)]$ is globally Lipschitz in $\xi_{i,k}(t)$ or $\|B[\xi_{i,k}(t)] - B[\xi_{j,k}(t)]\| \le c_B\|\xi_{i,k}(t) - \xi_{j,k}(t)\|$ for all $k \ge 0$, $t \in [0, T]$, $i \in \{1, 2, \ldots, n\}$ and for some positive constant c_B.

Property 2: The matrix $B[\xi_{i,k}(t)]$ is bounded as $\|B[\xi_{i,k}(t)]\| \le b_B$, where b_B is a positive constant. Furthermore, $CB[\xi_{i,k}(t)]$ is a full-column rank matrix.

Remark 1: Note that the above properties are also given in [37] for nonholonomic mobile robot. Further, we can note that the matrix $CB(k)$ has full-column rank rather than full-row rank and the number of system inputs is less than the number of system outputs, which leads to the dissatisfaction as assumption A3 stated in [32].

C. FORMATION CONTROL OBJECTIVE

In this paper, the formation control objective is to develop an appropriate algorithm such that a group of mobile robots track a reference trajectory while maintaining a desired geometric shape including positions and orientations. Specially, as stated in Section I.A, each robot v_i in the distributed directed graph network $\mathcal{G}$ can keep a desired deviation $d_i(t)$ from the virtual robot v_0 which creates the reference trajectory $r(t)$ for all time steps over a finite interval. That is, for $i \in \mathcal{I}_n$ and $t \in [0, T]$

$$\lim_{k\to\infty} \eta_{i,k}(t) = r(t) + d_i(t) = \eta_i^d(t) \tag{4}$$

In developing the controller, we impose two assumptions as follows:

Assumption 1: Suppose that the desired formation trajectory is not influenced by the disturbances and measurement

noises for $t \in [0, T]$. The desired formation trajectory for robot i at iterative learning algorithm design is given as $\eta_i^d(t)$, there exists a unique controller $u_i^d(t)$ that can control the mobile robot v_i to track $\eta_i^d(t)$ exactly, which can be represented as

$$\begin{cases} \xi_i^d(t+1) = \xi_i^d(t) + B[\xi_i^d(t)]u_i^d(t) \\ \eta_i^d(t) = C\xi_i^d(t), \xi_i^d(0) = \xi_{i0}^d \end{cases} \tag{5}$$

and the desired input $u_i^d(t)$ satisfies $\|u_i^d(t)\| \leq b_u$.

Assumption 2: For all $k \geq 0$, $t \in [0, T]$, the initial state errors, disturbances and measurement noises are bounded as $\|\xi_{i,k}(0) - \xi_i^d(0)\| \leq b_{\xi_0}, \|\varsigma_{i,k}(t)\| \leq b_\varsigma$, $\|\gamma_{i,k}(t)\| \leq b_\gamma$ where b_{ξ_0}, b_ς and b_γ are positive constants.

Remark 2: As in [37], we know that the desired formation trajectory is usually not influenced by the disturbances and measurement noises. Further, from [32] and [38], we know that the initial state errors, disturbances and measurement noises are bounded, so the Assumptions 1-2 are reasonable.

Note that the mobile robot is influenced by the bounded initial state shifts, disturbances, noises and communication delays, which causes the formation control objective (4) may not be accomplished accurately. Thus, we attempt to guarantee the trajectory tracking errors $e_{i,k}(t) = \eta_i^d(t) - \eta_{i,k}(t)$ of each mobile robot to reach to a certain bound for $i \in \mathcal{I}_n$ and $t \in [1, T]$

$$\limsup_{k\to\infty} \|e_{i,k}(t)\| \leq b_e \tag{6}$$

where $b_e \geq 0$ depends on b_{ξ_0}, b_ς and/or b_γ.

Denote the relative position and orientation formation between the robot v_i and robot v_j at kth iteration as $\eta_{ij,k}(t) = \eta_{i,k}(t) - \eta_{j,k}(t)$, and denote $d_{ij}(t) = d_i(t) - d_j(t)$ ($\eta_{ij}^d(t) = \eta_i^d(t) - \eta_j^d(t) = d_{ij}(t)$) as the desired relative formation from v_i to v_j. Then, it is clearly that if (6) is achieved, the formation tracking error also can be guaranteed. That is, for $i \in \mathcal{I}_n$ and $t \in [1, T]$, the formation tracking error $e_{ij,k}(t) = \eta_{ij}^d(t) - \eta_{ij,k}(t)$ satisfies

$$\limsup_{k\to\infty} \|e_{ij,k}(t)\| \leq b_\eta \tag{7}$$

where b_η is also a certain bound depending on b_{ξ_0}, b_ς and/or b_γ.

III. CONTROLLER DESIGN

A. CURRENT-ITERATION ITERATIVE LEARNING CONTROL

Incorporating current state feedback with open-loop ILC is an useful method to prevent transient tracking errors from increasing too large before convergence [22]. The general current-iteration ILC algorithm is given by

$$u_{k+1}(t) = u_k(t) + L_1 e_k(t+1) + L_2 e_{k+1}(t) \tag{8}$$

for the $k+1$th iteration and as shown in Fig.1. $e_{k+1}(t) = y_d(t) - y_{k+1}(t)$ is the output tracking error, and L_1 and L_2 are the learning gain matrices. The control signal consisting of both predictive learning term $u_k(t) + L_1 e_k(t+1)$ at time step $t+1$ that from the kth iteration information stored

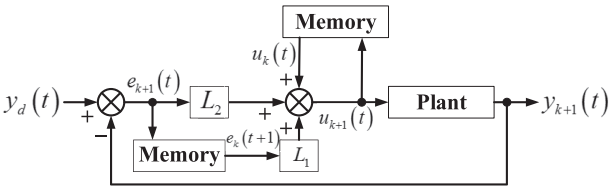

FIGURE 1. Current-iteration ILC architecture.

in memory and current learning term $L_2 e_{k+1}(t)$ that boosts system stability against unpredictable uncertainties.

B. ILC-BASED ALGORITHM DESIGN

In order to satisfy the formation control for the group of differential-drive mobile robots with communication delays under disturbances and noises environment, the distributed algorithm based on current-ILC scheme is presented as shown in Fig.2. Clearly, from this figure the algorithm is given by:

$$\begin{aligned} u_{i,k+1}(t) = {} & u_{i,k}(t) + \Gamma_{i,k}(t) \\ & \times \left\{ \sum_{j\in\mathcal{N}_i} a_{ij} e_{ij,k}(t+1) + a_{i0} e_{i,k}(t+1) \right\} \\ & + \Gamma'_{i,k+1}(t) \\ & \times \left\{ \sum_{j\in\mathcal{N}_i} a_{ij} \hat{e}_{ij,k+1}(t - \tau_{ij,k+1}(t)) \right. \\ & \left. + a_{i0} \hat{e}_{i,k+1}(t - \tau_{ii,k+1}(t)) \right\} \end{aligned} \tag{9}$$

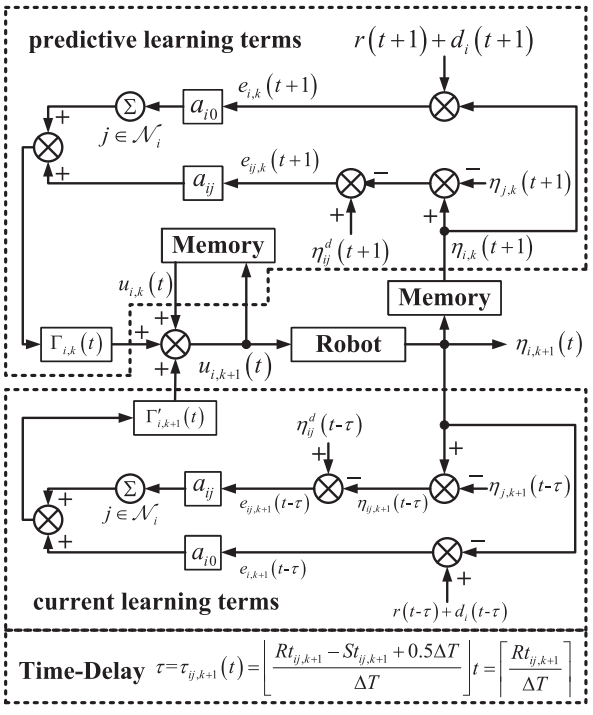

FIGURE 2. A diagram of the algorithm (9) performed for the robot i, $i \in \mathcal{I}_n$.

where $u_{i,0}(t)$ is the initial input for the robot v_i, and it can be selected arbitrarily, $\Gamma_{i,k}(t)$ and $\Gamma'_{i,k}(t) \in \mathbb{R}^{2\times 3}$ are the learning gain matrixes that satisfy $\|\Gamma_{i,k}(t)\| \leq b_\Gamma$ and $\|\Gamma'_{i,k}(t)\| \leq b_{\Gamma'}$, $\tau_{ij,k+1}(t)$ and $\tau_{ii,k+1}(t)$ are denote the communication time-delays from robot v_j to v_i and from robot v_0 to v_i at time t of $k+1$th iteration, respectively, $\hat{e}_{ij,k+1}(t)$ and $\hat{e}_{i,k+1}(t)$ satisfy

$$\hat{e}_{ij,k+1}(t) = \begin{cases} e_{ij,k+1}(t), & \text{if } t \geq 1 \\ 0, & \text{if } t \leq 0 \end{cases}$$
$$\hat{e}_{i,k+1}(t) = \begin{cases} e_{i,k+1}(t), & \text{if } t \geq 1 \\ 0, & \text{if } t \leq 0 \end{cases} \tag{10}$$

In particular, we assume that the mobile robots in the formation system have a synchronous clock. This assumption is reasonable because the synchronization protocols [39] can be used to synchronize the asynchronous clocks in the case of local internal clocks drift. Then we add the time-label for every communication information, and denote the sending time and the receiving time for the robot v_i receives information from robot v_j at time t of $k+1$ iteration as $St_{ji,k+1}$ and $Rt_{ij,k+1}$, respectively, and we can calculate the delay $\tau_{ij,k+1}(t)$ as the number of sampling periods:

$$\tau_{ij,k+1}(t) = \lfloor \frac{Rt_{ij,k+1} - St_{ji,k+1} + 0.5\Delta T}{\Delta T} \rfloor \tag{11}$$

It is worth noting that the delays only affect the current learning term in controller (9) since the predictive learning term can use the whole state information of its neighbor through memory rather than communication. Furthermore, it is reasonable to consider $0 \leq \tau_{ij,k+1}(t) \leq T$ due to $t \in [0, T]$. Hence, we can assume that $\tau_{ij,k+1}(t) \in [0, \tau_{\max}]$ with $\tau_{\max} < N$, and we can define

$$\hat{a}^d_{ij} = \begin{cases} a_{ij}, & \text{if } \tau_{ij,k+1}(t) = d \\ 0, & \text{otherwise} \end{cases}$$
$$\hat{a}^d_{i0} = \begin{cases} a_{i0}, & \text{if } \tau_{ij,k+1}(t) = d \\ 0, & \text{otherwise} \end{cases} \tag{12}$$

for any $d \in [0, \tau_{\max}]$, and $\hat{\mathcal{A}}^d = [\hat{a}^d_{ij}]$, $\hat{\Omega}^d = diag\{\hat{a}^d_{10}, \hat{a}^d_{20}, \ldots, \hat{a}^d_{n0}\}$. Then, with these definitions, we modify the controller (9):

$$\begin{aligned} u_{i,k+1}(t) &= u_{i,k}(t) + \Gamma_{i,k}(t) \\ &\times \left\{ \sum_{j\in\mathcal{N}_i} a_{ij} e_{ij,k}(t+1) + a_{i0} e_{i,k}(t+1) \right\} \\ &+ \Gamma'_{i,k+1}(t) \\ &\times \left\{ \sum_{j\in\mathcal{N}_i} \sum_{d=0}^{\tau_{\max}} \hat{a}^d_{ij} \hat{e}_{ij,k+1}(t-d) + \hat{a}^d_{i0} \hat{e}_{i,k+1}(t-d) \right\} \end{aligned} \tag{13}$$

C. CONVERGENCE ANALYSIS

With the help of the 2-D analysis approach and graph theory, the dynamic evolution and formation error convergence of the multi-robot system under the proposed algorithm (13) will be analyzed in this part. At first, we introduce the state error between kth iteration and desired values at time $t+1$:

$$\Delta\xi_{i,k}(t+1) = \xi^d_i(t+1) - \xi_{i,k}(t+1)$$

and introduce the output error between $k+1$th iteration and desired values at time $t+1$:

$$\Delta\eta_{i,k}(t+1) = \eta^d_i(t+1) - \eta_{i,k+1}(t+1)$$

And input error between $k+1$th iteration and desired values at time t:

$$\Delta u_{i,k+1}(t) = u^d_i(t) - u_{i,k+1}(t)$$

Then by noting the assumption 1, deduce from (3), (5) and (13), we can get the error equations (14)–(16), as shown at the top of the next page, where $f(\Delta\xi_{i,k}(t)) = \Delta\xi_{i,k}(t) + [B[\xi^d_i(t)] - B[\xi_{i,k}(t)]]u^d_i(t)$ and $g(\Delta\eta_{i,k}(t)) = \Delta\eta_{i,k}(t) + [B[\eta^d_i(t)] - B[\eta_{i,k+1}(t) - \gamma_{i,k+1}(t)]]u^d_i(t)$.

It can be easily seen that the equations (14), (15) and (16) describe the dynamic evolution along both a finite time axis and an infinite iteration axis of state error, output error and input error, respectively. This reflects the fundamental 2-D dynamic process and makes the 2-D analysis approach (for a 2-D Roesser system) suitable for the convergence analysis. Motivated by this observation, we denote

$$\begin{aligned} \Delta\xi_k(t) &= [\Delta\xi^{\mathrm{T}}_{1,k}(t), \Delta\xi^{\mathrm{T}}_{2,k}(t), \ldots, \Delta\xi^{\mathrm{T}}_{n,k}(t)]^{\mathrm{T}} \\ \Delta u_k(t) &= [\Delta u^{\mathrm{T}}_{1,k}(t), \Delta u^{\mathrm{T}}_{2,k}(t), \ldots, \Delta u^{\mathrm{T}}_{n,k}(t)]^{\mathrm{T}} \\ \Delta\eta_k(t) &= [\Delta\eta^{\mathrm{T}}_{1,k}(t), \Delta\eta^{\mathrm{T}}_{2,k}(t), \ldots, \Delta\eta^{\mathrm{T}}_{n,k}(t)]^{\mathrm{T}} \\ \Delta\hat{\eta}_k(t) &= [\Delta\hat{\eta}^{\mathrm{T}}_{1,k}(t), \Delta\hat{\eta}^{\mathrm{T}}_{2,k}(t), \ldots, \Delta\hat{\eta}^{\mathrm{T}}_{n,k}(t)]^{\mathrm{T}} \\ F(\Delta\xi_k(t)) &= [f^{\mathrm{T}}(\Delta\xi_{1,k}(t)), f(\Delta\xi_{2,k}(t))^{\mathrm{T}}, \\ &\quad \ldots, f(\Delta\xi_{n,k}(t))^{\mathrm{T}}]^{\mathrm{T}} \\ G(\Delta\eta_k(t)) &= [g^{\mathrm{T}}(\Delta\eta_{1,k}(t)), g(\Delta\eta_{2,k}(t))^{\mathrm{T}}, \\ &\quad \ldots, g(\Delta\eta_{n,k}(t))^{\mathrm{T}}]^{\mathrm{T}} \\ \varsigma_k(t) &= [\varsigma^{\mathrm{T}}_{1,k}(t), \varsigma^{\mathrm{T}}_{2,k}(t), \ldots, \varsigma^{\mathrm{T}}_{n,k}(t)]^{\mathrm{T}} \\ \gamma_k(t) &= [\gamma^{\mathrm{T}}_{1,k}(t), \gamma^{\mathrm{T}}_{2,k}(t), \ldots, \gamma^{\mathrm{T}}_{n,k}(t)]^{\mathrm{T}} \\ B_k(t) &= diag\{B[\xi_{1,k}(t)], B[\xi_{2,k}(t)], \cdots, B[\xi_{n,k}(t)]\} \\ \Gamma_k(t) &= diag\{\Gamma[\xi_{1,k}(t)], \Gamma[\xi_{2,k}(t)], \cdots, \Gamma[\xi_{n,k}(t)]\} \end{aligned}$$

and then we can rewrite (14), (15) and (16) in a compact form of

$$\begin{aligned} \Delta\xi_k(t+1) &= F(\Delta\xi_k(t)) + B_k(t)\Delta u_k(t) - B_k(t)\varsigma_k(t) \\ \Delta u_{k+1}(t) &= \Delta u_k(t) \\ &\quad - \sum_{d=0}^{\tau_{\max}} [(\mathcal{L}_{\hat{\mathcal{A}}^d} + \hat{\Omega}^d) \otimes I_2]\Gamma'_{k+1}(t)\Delta\hat{\eta}_k(t-d) \\ &\quad - [(\mathcal{L}_{\mathcal{A}} + \Omega) \otimes I_2]\Gamma_k(t)\Delta\xi_k(t+1) \\ &\quad + [(\mathcal{L}_{\mathcal{A}} + \Omega) \otimes I_2]\Gamma_k(t)\gamma_k(t+1) \\ \Delta\eta_k(t+1) &= G(\Delta\eta_k(t)) + B_{k+1}(t)\Delta u_{k+1}(t) \\ &\quad - B_{k+1}(t)\varsigma_k(t) - \gamma_{k+1}(t+1) + \gamma_{k+1}(t) \end{aligned} \tag{17}$$

$$\begin{aligned}\Delta\xi_{i,k}(t+1) &= \xi_i^d(t+1) - \xi_{i,k}(t+1)\\ &= f(\Delta\xi_{i,k}(t)) + B[\xi_{i,k}(t)]\Delta u_{i,k}(t) - B[\xi_{i,k}(t)]\varsigma_{i,k}(t) \qquad (14)\\ \Delta u_{i,k+1}(t) &= u_i^d(t) - u_{i,k+1}(t)\\ &= \Delta u_{i,k}(t) - \Gamma'_{i,k+1}(t)\Big\{\sum_{j\in\mathcal{N}_i}\sum_{d=0}^{\tau_{\max}}\hat{a}_{ij}^d[\Delta\hat{\eta}_{i,k}(t-d) - \Delta\hat{\eta}_{j,k}(t-d)] + \hat{a}_{i0}^d[\Delta\hat{\eta}_{i,k}(t-d)]\Big\}\\ &\quad - \Gamma_{i,k}(t)\Big\{\sum_{j\in\mathcal{N}_i} a_{ij}[\Delta\xi_{i,k}(t+1) - \Delta\xi_{j,k}(t+1)] + a_{i0}\Delta\xi_{i,k}(t+1)\Big\}\\ &\quad - \Gamma_{i,k}(t)\Big\{\sum_{j\in\mathcal{N}_i} a_{ij}[\gamma_{j,k}(t+1) - \gamma_{i,k}(t+1)] - a_{i0}\gamma_{i,k}(t+1)\Big\} \qquad (15)\\ \Delta\eta_{i,k}(t+1) &= \eta_i^d(t+1) - \eta_{i,k+1}(t+1)\\ &= \Delta\eta_{i,k}(t) + B[\eta_i^d(t)]u_i^d(t) - B[\eta_{i,k+1}(t) - \gamma_{i,k+1}(t)]u_{i,k+1}(t)\\ &\quad - \{B[\xi_{i,k+1}(t)]\varsigma_{i,k+1}(t) + \gamma_{i,k+1}(t+1) - \gamma_{i,k+1}(t)\}\\ &= g(\Delta\eta_{i,k}(t)) + B[\xi_{i,k+1}(t)]\Delta u_{i,k+1}(t) - \{B[\xi_{i,k+1}(t)]\varsigma_{i,k+1}(t) + \gamma_{i,k+1}(t+1) - \gamma_{i,k+1}(t)\} \qquad (16)\end{aligned}$$

Consequently, for the equation (17), we substitute the first line into the second line, the second line into the third line, and denote,

$$\begin{aligned}\Xi &= [(\mathcal{L}_{\mathcal{A}} + \Omega)\otimes I_2]\\ \hat{\Xi}^d &= [(\mathcal{L}_{\hat{\mathcal{A}}^d} + \hat{\Omega}^d)\otimes I_2]\\ \Theta_{11,k}(t) &= F(\Delta\xi_k(t))\\ \Theta_{12,k}(t) &= O_{3n\times 3n}\\ \Theta_{13,k}(t) &= O_{3n\times 3n}\\ \Theta_{14,k}(t) &= B_k(t)\Delta u_k(t)\\ \Theta_{21,k}(t) &= -B_{k+1}(t)\Xi\Gamma_k(t)F(\Delta\xi_k(t))\\ \Theta_{22,k}(t) &= G(\Delta\eta_k(t))\\ \Theta_{23,k}(t) &= -B_{k+1}(t)\sum_{d=0}^{\tau_{\max}}\hat{\Xi}^d\Gamma'_k(t)\Delta\hat{\eta}_k(t-d)\\ \Theta_{24,k}(t) &= B_{k+1}(t)[I_{2n} - \Xi\Gamma_k(t)B_k(t)]\Delta u_k(t)\\ \Theta_{31,k}(t) &= -\Xi\Gamma_k(t)F(\Delta\xi_k(t))\\ \Theta_{32,k}(t) &= O_{3n\times 3n}\\ \Theta_{33,k}(t) &= -\sum_{d=0}^{\tau_{\max}}\hat{\Xi}^d\Gamma'_k(t)\Delta\hat{\eta}_k(t-d)\\ \Theta_{34,k}(t) &= (I_{2n} - \Xi\Gamma_k(t)B_k(t))\Delta u_k(t)\\ \Upsilon_{1,k}(t) &= -B_k(t)\varsigma_k(t)\\ \Upsilon_{2,k}(t) &= B_{k+1}(t)\Xi\Gamma_k(t)B_k(t)\varsigma_k(t) + B_{k+1}(t)\Xi\Gamma_k(t)\gamma_k(t+1)\\ &\quad - B_{k+1}(t)\varsigma_k(t) - \gamma_{k+1}(t+1) + \gamma_{k+1}(t)\\ \Upsilon_{3,k}(t) &= \Xi\Gamma_k(t)B_k(t)\varsigma_k(t) + \Xi\Gamma_k(T)\gamma_k(t+1)\end{aligned}$$

we can gain a 2D Roesser system as

$$\begin{aligned}\Delta\xi_k(t+1) &= \Theta_{11,k}(t) + \Theta_{12,k}(t) + \Theta_{13,k}(t)\\ &\quad + \Theta_{14,k}(t) + \Upsilon_{1,k}(t)\\ \Delta\eta_k(t+1) &= \Theta_{21,k}(t) + \Theta_{22,k}(t) + \Theta_{23,k}(t)\\ &\quad + \Theta_{24,k}(t) + \Upsilon_{2,k}(t)\\ \Delta u_{k+1}(t) &= \Theta_{31,k}(t) + \Theta_{32,k}(t) + \Theta_{33,k}(t)\\ &\quad + \Theta_{34,k}(t) + \Upsilon_{3,k}(t) \qquad (18)\end{aligned}$$

Then, in order to obtain the the ultimately bounded convergence result for the 2-D Roesser system (18), we first propose the following convergence result.

Lemma 1: Given $\Delta\xi_k(t)$, $\Delta\eta_k(t)$ and $\Delta u_k(t)$ over $t \in [0, T]$ and $k \in \mathbb{Z}_+$, if there exist nonnegative scalars $b_1 \geq 0$, $b_2 \geq 0$, $b_3 \geq 0$, $b_4 \geq 0$, $b_5 \geq 0$, $b_6 \geq 0$, $\theta_{11} \geq 0$, $\theta_{12} \geq 0$, $\theta_{13} \geq 0$, $\theta_{14} \geq 0$, $\theta_{21} \geq 0$, $\theta_{22} \geq 0$, $\theta_{23} \geq 0$, $\theta_{24} \geq 0$, $\theta_{31} \geq 0$, $\theta_{32} \geq 0$, $\theta_{33} \geq 0$, and $0 \leq \theta_{34} < 1$, such that

$$\begin{aligned}\|\Delta\xi_k(t+1)\| &\leq \theta_{11}\|\Delta\xi_k(t)\| + \theta_{12}\|\Delta\eta_k(t)\|\\ &\quad + \theta_{13}\sum_{d=0}^{\tau_{\max}}\|\Delta\hat{\eta}_k(t-d)\|\\ &\quad + \theta_{14}\|\Delta u_k(t)\| + b_1\\ \|\Delta\eta_k(t+1)\| &\leq \theta_{21}\|\Delta\xi_k(t)\| + \theta_{22}\|\Delta\eta_k(t)\|\\ &\quad + \theta_{23}\sum_{d=0}^{\tau_{\max}}\|\Delta\hat{\eta}_k(t-d)\|\\ &\quad + \theta_{24}\|\Delta u_k(t)\| + b_2\\ \|\Delta u_{k+1}(t)\| &\leq \theta_{31}\|\Delta\xi_k(t)\| + \theta_{32}\|\Delta\eta_k(t)\|\\ &\quad + \theta_{33}\sum_{d=0}^{\tau_{\max}}\|\Delta\hat{\eta}_k(t-d)\|\\ &\quad + \theta_{34}\|\Delta u_k(t)\| + b_3\\ \|\Delta\xi_k(0)\| &\leq b_4, \quad \|\Delta\eta_k(0)\| \leq b_5, \quad \|\Delta u_0(t)\| \leq b_6 \qquad (19)\end{aligned}$$

where

$$\Delta\hat{\eta}_k(t) = \begin{cases}\Delta\eta_k(t), & \text{if } t \geq 1\\ 0, & \text{if } t \leq 0\end{cases},$$

then $\limsup_{k\to\infty} \|\Delta\xi_k(t)\| \le b_7$, $\limsup_{k\to\infty} \|\Delta\eta_k(t)\| \le b_8$ and $\limsup_{k\to\infty} \|\Delta u_k(t)\| \le b_9$ for $t \in [1, T]$, where $b_7 \ge 0$, $b_8 \ge 0$ and $b_9 \ge 0$ are a certain bound depending on b_1, b_2, b_3, b_4 and/or b_5

In Appendix A, we give the proof of Lemma 1. It is observable that (19) sets up a 2-D Rosser system regarding $\xi_k(t)$, $\eta_k(t)$ as well as $u_k(t)$. It suggests that the ultimately bounded convergence is attained in respect of 2-D Roesser systems using time-changing as well as iteration-changing matrix parameters. In addition to that, using Lemma 1, we are capable of proposing the following performance associated development outcome regarding multi-robot systems.

Theorem 1: For the multi-robot system (3) linked to the directed graph $\mathcal{G}$, in a case that the distributed algorithm (9) is put to application with the gain matrix $\Gamma_k(t)$ providing satisfaction, in respect of all $t \in [0, T]$ and $k \in \mathbb{Z}_+$

$$\|I_{2n} - [(\mathcal{L}_{\mathcal{A}} + \Omega) \otimes I_2] \times \Gamma_k(t) B_k(t)\| \le b_c < 1 \quad (20)$$

thereafter, the development aim (7) is able to be attained.

Proof: Based on the Property 1 and Assumption 2, we can yield:

$$\|F(\Delta\xi_k(t))\| \le (1 + c_B b_u)\|\Delta\xi_k(t)\|$$
$$\|G(\Delta\eta_k(t))\| \le (1 + c_B b_u)\|\Delta\eta_k(t)\| + c_B b_u b_\gamma$$

Note also that Ω is the weight matrix associated with the accessibility of virtue leader for the robots in $\mathcal{G}$, Thus, the uniform boundedness of $(\mathcal{L}_{\mathcal{A}}+\Omega)\otimes I_2$ and $(\mathcal{L}_{\hat{\mathcal{A}}^d}+\hat{\Omega}^d)\otimes I_2$ can be guaranteed, which denotes as $\|\Xi\| = \|(\mathcal{L}_{\mathcal{A}}+\Omega)\otimes I_2\| \le b_{\Xi 1}$ and $\|\hat{\Xi}^d\| = \|(\mathcal{L}_{\hat{\mathcal{A}}^d} + \hat{\Omega}^d) \otimes I_2 \otimes I_2\| \le b_{\Xi 2}$.

Then, by noting the notation in (18) and convergence condition (20), we can derive

$$\|\Theta_{11,k}(t)\| \le \theta_{11}\|\Delta\xi_k(t)\|$$
$$\|\Theta_{12,k}(t)\| \le \theta_{12}\|\Delta\eta_k(t)\|$$
$$\|\Theta_{13,k}(t)\| \le \theta_{13}\sum_{d=0}^{\tau_{\max}}\|\Delta\hat{\eta}_k(t-d)\|$$
$$\|\Theta_{14,k}(t)\| \le \theta_{14}\|\Delta u_k(t)\|$$
$$\|\Theta_{21,k}(t)\| \le \theta_{21}\|\Delta\xi_k(t)\|$$
$$\|\Theta_{22,k}(t)\| \le \theta_{22}\|\Delta\eta_k(t)\|$$
$$\|\Theta_{23,k}(t)\| \le \theta_{23}\sum_{d=0}^{\tau_{\max}}\|\Delta\hat{\eta}_k(t-d)\|$$
$$\|\Theta_{24,k}(t)\| \le \theta_{24}\|\Delta u_k(t)\|$$
$$\|\Theta_{31,k}(t)\| \le \theta_{31}\|\Delta\xi_k(t)\|$$
$$\|\Theta_{32,k}(t)\| \le \theta_{32}\|\Delta\eta_k(t)\|$$
$$\|\Theta_{33,k}(t)\| \le \theta_{33}\sum_{d=0}^{\tau_{\max}}\|\Delta\hat{\eta}_k(t-d)\|$$
$$\|\Theta_{34,k}(t)\| \le \theta_{34}\|\Delta u_k(t)\|$$
$$\|\Upsilon_{1,k}(t)\| \le b_1$$
$$\|\Upsilon_{2,k}(t)\| \le b_2$$
$$\|\Upsilon_{3,k}(t)\| \le b_3$$

where $\theta_{34} = \|I_{2n} - [(\mathcal{L}_{\mathcal{A}} + \Omega) \otimes I_2] \times \Gamma_k(t)B_k(t)\|$ and $0 \le \theta_{34} < 1$, moreover, $\theta_{11} = 1 + c_B b_u$, $\theta_{12} = 0$, $\theta_{13} = 0$, $\theta_{14} = b_B$, $\theta_{21} = b_B b_{\Xi 1} b_\Gamma(1 + c_B b_u)$, $\theta_{22} = 1 + c_B b_u$, $\theta_{23} = b_B b_{\Xi 2} b_{\Gamma'}$, $\theta_{24} = b_B\theta_{34}$, $\theta_{31} = b_{\Xi 1} b_\Gamma(1 + c_B b_u)$, $\theta_{32} = 0$, $\theta_{33} = b_{\Xi 2} b_{\Gamma'}$, $\theta_{34} = 1 + b_{\Xi 1} b_\Gamma b_B$, $b_1 = b_B b_\varsigma$, $b_2 = b_B b_{\Xi 1} b_\Gamma(b_B b_\varsigma + b_\gamma) + b_B b_\varsigma + 2b_\gamma + c_B b_u b_\gamma$, $b_3 = b_{\Xi 1} b_\Gamma(b_B b_\varsigma + b_\gamma)$ $b_4 = b_{\xi_0}$, $b_5 = b_{\xi_0} + b_\gamma$.

Furthermore, according to the assumptions 1 and 2, and choosing a bounded initial input $u_{i,0}(t)$ likes $u_{i,0}(t) = 0$, we can have $\|\Delta\xi_k(0)\| \le b_{\xi_0}$, $\|\Delta\eta_k(0)\| \le b_{\xi_0} + b_\gamma$, $\|\Delta u_0(t)\| \le b_u$. Then according to lemma 1, $\limsup_{k\to\infty} \|\Delta\xi_k(t)\|$, $\limsup_{k\to\infty} \|\Delta\eta_k(t)\|$ and $\limsup_{k\to\infty} \|\Delta u_k(t)\|$ will be ultimately bounded with bounds that are functions of b_{ξ_0} , b_ς , and b_γ at $t \in [1, T]$, which means the formation objective (7) can be achieved. ■

Remark 3: Theorem (1) shows that the differential-drive mobile robots formation can be realized in the realistic situation involving initial state shifts, disturbances, noises, and communication time-delays. Furthermore, the convergence condition is only depend on the learning gain matrix $\Gamma_{i,k}(t)$, which means the learning gain matrix is mainly affected the transient tracking errors rather than the ultimate tracking errors. The simulation results in Section IV show this conclusion.

As presented by the Theorem 1, it is evident to us that the matrix norm condition (20) performs a quintessential function in getting their convergence findings in respect of multi-robot development jobs. In addition, convergence state is dependent on the network topology information of the contact between the robots. As a result, whether the condition (20) can be met or not is essentially needed to be taken into consideration. It provides us with motivation for the establishment of an essential prerequisite in the subsequent theorem for attaining the convergence state (20).

Theorem 2: Provided $t \in [0, T]$ and $k \in \mathbb{Z}_+$, there can be discovered a gain matrix $\Gamma_k(t)$ that satisfies the condition (20) only if the directed graph $\tilde{\mathcal{G}}$ contains a spanning tree.

Proof: We develop this proof by using the proof by contradiction.

Suppose that the directed graph $\tilde{\mathcal{G}}$ does not contain a spanning tree, subsequently, we can obtain a conclusion from [40, Lemma 3.3] that $[\mathcal{L}_{\mathcal{A}} + \Omega] \otimes I_2$ contains a minimum of one zero eigenvalue.

Hence, $I_{2n} - [(\mathcal{L}_{\mathcal{A}} + \Omega) \otimes I_2$ has at least one eigenvalue that is equal to one. This can lead to

$$\|I_{2n} - [(\mathcal{L}_{\mathcal{A}} + \Omega) \otimes I_2\| \ge \rho(I_{2n} - [(\mathcal{L}_{\mathcal{A}} + \Omega) \otimes I_2) = 1 \quad (21)$$

which is a contradiction with (20) can be obtained. ■

IV. SIMULATION AND EXPERIMENT STUDIES

A. SIMULATION

In this section, a numerical example is provided to verify the proposed algorithm. The multi-robot system considered in this part is a six-robot system, and the reference trajectory

is set as

$$r(t) = \begin{bmatrix} x_r(t) \\ y_r(t) \\ \theta_r(t) \end{bmatrix} = \begin{bmatrix} 7.5\sin(2\pi t\Delta T/45) \\ 10\sin(4\pi t\Delta T/45) \\ \arctan\left(\dfrac{8\cos(4\pi t\Delta T/45)}{3\cos(2\pi t\Delta T/45)}\right) \end{bmatrix}$$

for $t \in [0, 300]$ and $\Delta T = 0.1s$, it takes 30s to complete one iteration. The simulation objective is to enable these six mobile robots to track the reference trajectory while maintaining the regular hexagon formation as Fig. 3. The distance between the robot v_i and virtue robot v_0 is denoted by $s(t)$, which is varies dynamically with respect to the time step. In this example, we consider $s(t) = 1 + 0.5\sin(4\pi t\Delta T/45)$, and then the desired formation trajectory of these six robots system is shown in Fig. 4, where the red arrow is the moving direction.

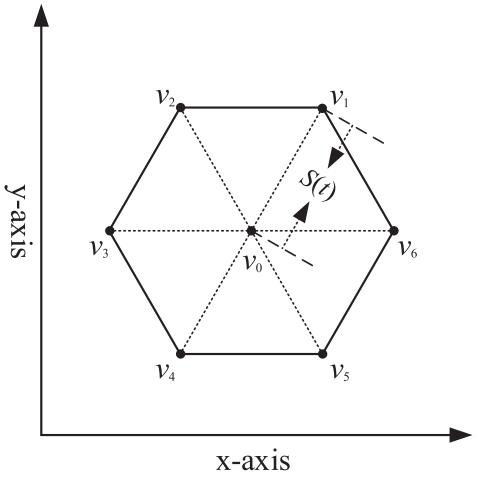

FIGURE 3. The desired geometric formation shape of the six-robot system in the Euclidean plane.

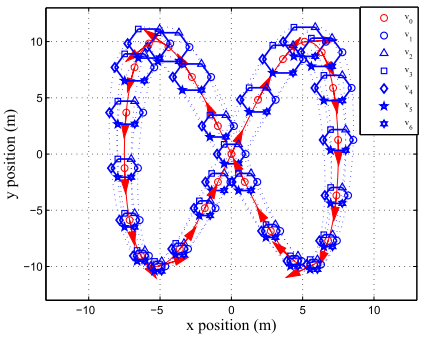

FIGURE 4. Desired formation trajectory of the six-robot system in the Euclidean plane.

The communication directed graph of this six-robot system is shown in Fig.5, It can be validated that $\tilde{\mathcal{G}}$ has a spanning tree. The delays are assumed to be evenly distributed from 0 to $3\Delta T$ ($0 \sim 0.3s$), i.e. $\tau_{ij,k} \in \{1, 2, 3, 4\}$. To simulate the dynamic changing of the communication delay along time axis and iteration axis, we define $\kappa(t, k)$ as a function of

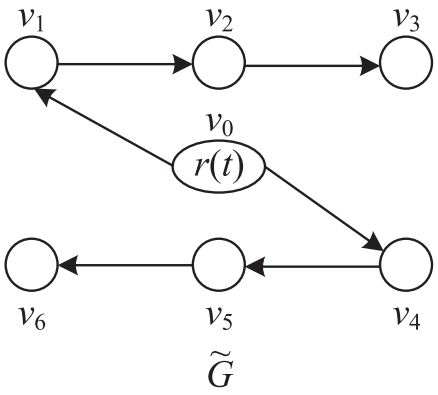

FIGURE 5. Directed graph $\tilde{\mathcal{G}}$ with six controlled robots and a virtual robot, and the weight of this directed graphs is 1.

both time variable t and iteration variable k, and set this signal varying over the interval [0, 1] by using the MATLAB command 'rand'. The delay is distributed as follows:

1) If $\kappa(t, k) \in [0, 0.15)$ and $\kappa(t, k) = 1$, then $\tau_{ij,k} = 1$.
2) If $\kappa(t, k) \in [0.15, 0.45)$ then $\tau_{ij,k} = 2$.
3) If $\kappa(t, k) \in [0.45, 0.8)$ then $\tau_{ij,k} = 3$.
4) If $\kappa(t, k) \in [0.8, 1)$ then $\tau_{ij,k} = 4$.

The initial states, disturbances and measurement noises of the ith differential driving mobile robot at the kth iteration take the form of

$$\begin{aligned} \xi_{i,k}(0) &= \xi_i^d(0) + \delta_{\xi_{i,k}} \\ \varsigma_{i,k}(t) &= \varsigma(t) + \delta_{\varsigma_{i,k}}(t) \\ \gamma_{i,k}(t) &= \gamma(t) + \delta_{\gamma_{i,k}}(t) \end{aligned}$$

where $\xi_i^d(0)$ is the desired initial states according to the formation task, $\delta_{\xi_{i,k}} = [\delta_{x_{i,k}}, \delta_{y_{i,k}}, \delta_{\theta_{i,k}}]^T$ is the initial state error varying along iteration axis, its elements $\delta_{x_{i,k}}$ and $\delta_{y_{i,k}}$ varying over the interval $[-0.05, 0.05]$, $\delta_{\theta_{i,k}}$ varying over the interval $[-(0.05/180)\pi, (0.05/180)\pi]$. $\varsigma(t)$ and $\gamma(t)$ are the iteration independent disturbances and measurements noises:

$$\begin{aligned} \varsigma(t) &= [0.01\sin(0.02t), (0.05/180)\pi\cos(0.02t)]^T \\ \gamma(t) &= [0.025\sin(0.03t), 0.025\sin(0.03t), \\ &\quad \times (0.1/180)\pi\cos(0.05t)]^T \end{aligned}$$

$\delta_{\varsigma_{i,k}}(t) = [\delta_{Dv_{i,k}}(t), \delta_{D\omega_{i,k}}(t)]^T$ and $\delta_{\gamma_{i,k}}(t) = [\delta_{Nx_{i,k}}(t), \delta_{Ny_{i,k}}(t), \delta_{N\theta_{i,k}}(t)]^T$ are the iteration varying disturbances and measurements noises, and the elements $\delta_{Dv_{i,k}}(t)$ varying over the interval $[-0.01, 0.01]$, $\delta_{D\omega_{i,k}}(t)$ varying over the interval $[-(0.1/180)\pi, (0.1/180)\pi]$, $\delta_{Nx_{i,k}}(t)$ and $\delta_{Ny_{i,k}}(t)$ varying over the interval $[-0.025, 0.025]$, $\delta_{N\theta_{i,k}}(t)$ varying over the interval $[-(0.1/180)\pi, (0.1/180)\pi]$. These varying functions are simulated using the MATLAB command 'rand'. In addition, we set the initial input of robot v_i is $u_{i,0}(t) \equiv 0$ for all t.

From Theorem 1, the algorithm (9) with the gain matrix $\Gamma_{i,k}(t)$ is chosen as

$$\Gamma_{i,k}(t) = 0.08\begin{bmatrix} \cos(\theta_{i,k}(t)) & \sin(\theta_{i,k}(t)) & 0 \\ 0 & 0 & 1 \end{bmatrix}$$

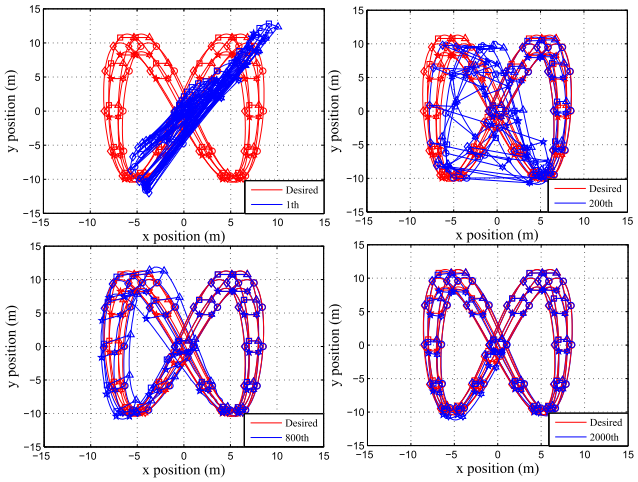

FIGURE 6. Tracking performance of robots at 1th, 100th, 200th, 300th and 1000th iteration.

And check the matrix norm condition (20):

$$\|I_{2n} - [(\mathcal{L}_{\mathcal{A}} + \Omega) \otimes I_2] \times \Gamma_k(t) B_k(t)\| \leq 0.9783 < 1$$

for all $t \in [0, T]$ and $k \in \mathbb{Z}_+$. Moreover, we chosen $\Gamma'_{i,k}(t) = \Gamma_{i,k}(t)$ for convenience.

Fig.6 shows the simulation results about the output trajectories of the six mobile robots after the $k = 1$, $k = 200$, $k = 800$ and $k = 2000$ iterations. It can be observed from Fig.6 that the formation tracking performance is improved as iteration increases.

To illustrate the importance of the current learning term and delay compensation in (9), we repeated the same simulation tests but with the control schemes:

$$u_{i,k+1}(t) = u_{i,k}(t) + \Gamma_{i,k}(t) \times \left\{ \sum_{j \in \mathcal{N}_i} a_{ij} e_{ij,k}(t+1) + a_{i0} e_{i,k}(t+1) \right\} \quad (22)$$

$$\begin{aligned} u_{i,k+1}(t) = {} & u_{i,k}(t) + \Gamma_{i,k}(t) \\ & \times \left\{ \sum_{j \in \mathcal{N}_i} a_{ij} [\eta^d_{ij}(t+1) - \eta_{ij,k}(t+1)] \right. \\ & \left. + a_{i0} [r(t+1) + d_i(t+1) - \eta_{i,k}(t+1)] \right\} \\ & + \Gamma'_{i,k+1}(t) \\ & \times \left\{ \sum_{j \in \mathcal{N}_i} a_{ij} [\eta^d_{ij}(t) - (\eta_{i,k+1}(t) \right. \\ & - \eta_{i,k+1}(t - \tau_{ij,k+1}(t)))] \\ & \left. + a_{i0} [\eta^d_i(t - \tau_{ii,k+1}(t)) - \eta_{i,k+1}(t)] \right\} \end{aligned} \quad (23)$$

where controller (22) contains only predictive learning terms and controller (23) ignores the affect of time delay.

The max position and orientation errors of the formation system under controller (9), (22) and (23) over the 2000 iterations are shown in Fig.7. It can be observed from this figure that the controller (23) is useless since time delay is ignored, and the controller (22) has the same convergence results as controller (9) after 1600th iterations, but with larger transient tracking errors and slower convergence speed. Furthermore, we can observe that the tracking errors of controller (9) and controller (22) are both decreased to vary within a small bound because of the initial state shifts, disturbances and measurements noises, which is equivalent to the conclusion of the theorem 1.

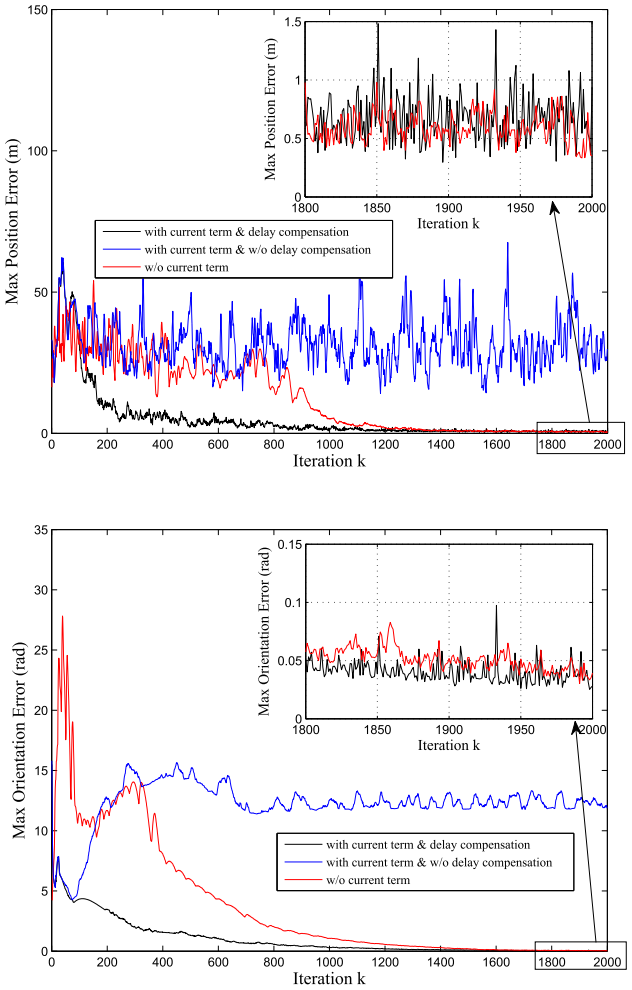

FIGURE 7. The maximum absolute position and orientation error of the six mobile robots system along iteration axis, black line(controller(9)), blue line(controller(22)) and red line(controller(23)).

B. EXPERIMENT

To further verify the effectiveness of applying the proposed distributed learning algorithm (9) to real formation task, we conduct a experiment using three actual mobile robots.

The experimental platform consists of three Pioneer 3-DX differential-drive mobile robots as shown in Fig.8. These robots are manufactured by Adept Inc, and can directly respond to linear and angular velocity commands. The formation task involves four application programs, one is the center server running on the base station personal computer (PC)

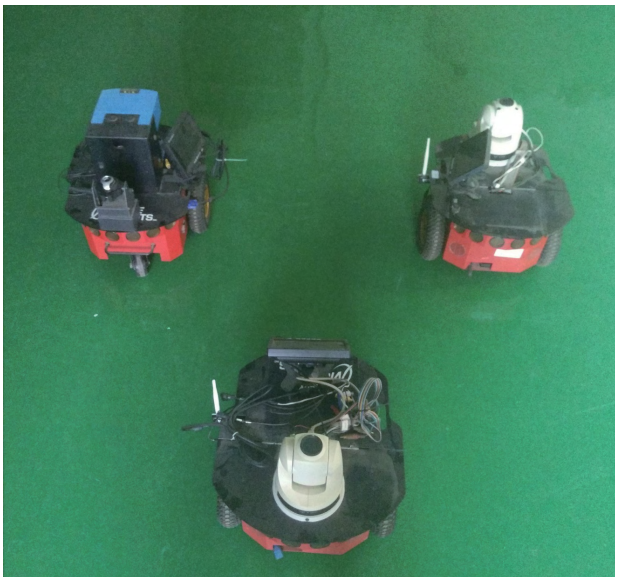

FIGURE 8. Poineer 3-DX mobile robots experimental platform.

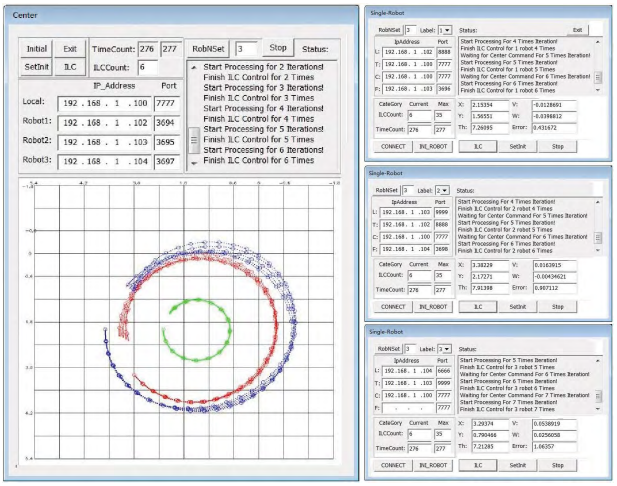

FIGURE 9. Application program interfaces of center server and robot controller.

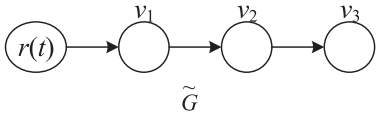

FIGURE 10. Directed graph $\tilde{\mathcal{G}}$ with three controlled robots and a virtual robot, and the weight of this directed graphs is 1.

which acts as the virtual robot, and the other three are running on the mobile robots which control the motion of the robot, the sample time ΔT of these programs is set as $0.2s$. In special, with the optical encoders installed on the driving motor axes and the camera mounted on the robot, self-localization for mobile robots in experimental environment can be realized by using the ceiling vision and the odometry method (see more detail in [29]), which is used to provide the position and orientation of the robot in the ground. These programs communication with each other via TCP/IP protocol over a WiFi network, and the interfaces of these programs are shown in Fig.9, and the communication directed graph of this three-robots system is shown in Fig.10. The total time of one iteration is set as $28s$, i.e. $t \in [0, 140]$ because $\Delta T = 0.2s$. and the linear and angular velocity of the virtual robot are set as

$$v_0(t) = \begin{cases} 0.35\dfrac{16-(t*0.2-4)^2}{16}, & \text{if } 0 \le t \le 20 \\ 0.35 & \text{if } 20 < t < 120 \\ 0.35\dfrac{16-(t*0.3-24)^2}{16}, & \text{if } 120 \le t \le 140 \end{cases}$$

$$w_0(t) = v_0(t)/1.5$$

which means the motion trajectory of virtual robot is a circle of radius $1.5m$, and the start velocity and stop velocity are set as zero to gain a good dynamic performance.

The desired geometric formation shape of the three-robot system in the form of a isosceles triangle in the virtual robot body coordinate is shown in Fig.11, where the time-varying distances between the robot v_i and virtual robot v_0 are denoted by $D_1(t)$ and $D_2(t)$, and

$$D_1(t) = 1 + 0.2\cos(t * 2\pi/28)$$
$$D_2(t) = 0.6 + 0.1\cos(t * 2\pi/28)$$

With these setting, the desired formation trajectory of these three robots system is shown in Fig.12.

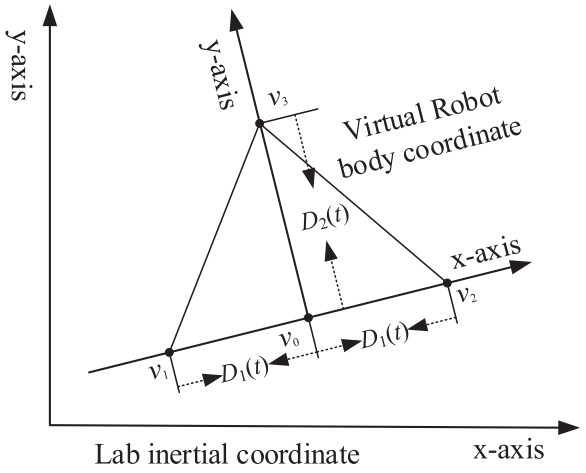

FIGURE 11. The desired geometric formation shape of the three-robot system.

At the initial stage of experimental tests, we performed the simulation tests for the first 300 iterations to generate the initial controller for the real robot, and we do not take the initial state shifts, disturbances, measurements noises and time-delays into account at this stage. Then the controller trained from simulation is applied to the real robots and Fig.13 shows the flow chart of the programs:

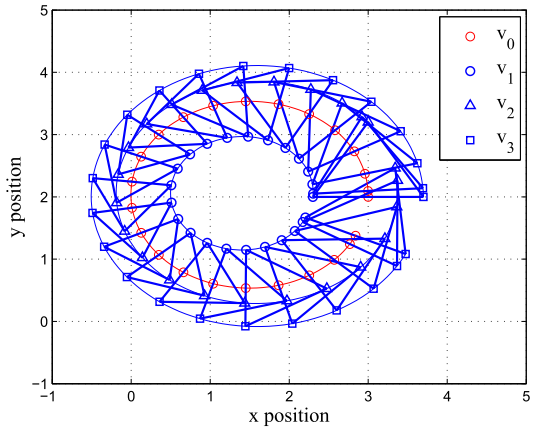

FIGURE 12. Desired formation trajectory of the three-robot system in the Euclidean plane.

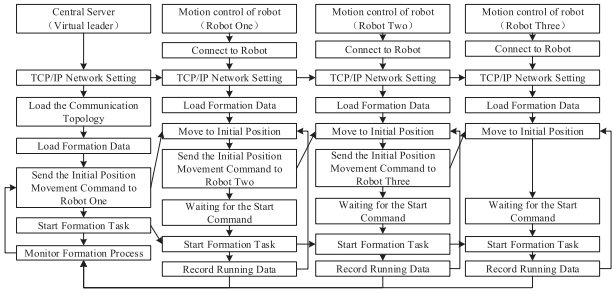

FIGURE 13. Flow chart of the programs.

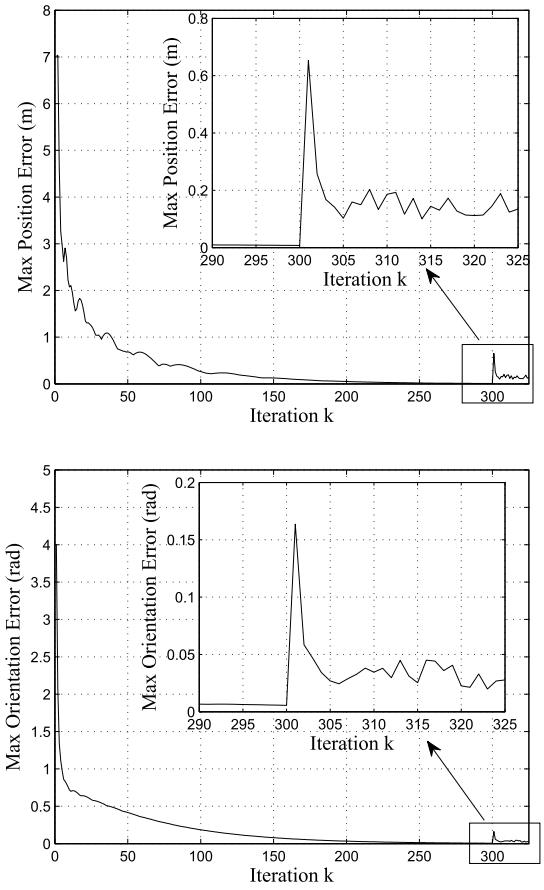

FIGURE 14. The maximum absolute position and orientation errors.

1) Set TCP/IP Network according to the communication topology;

2) Each robot move to the initial position via a point stabilization controller [30];

3) Start formation task, the controller (9) is applied to generate the control input for the mobile robot at each sample period;

4) Record the running data, and restart again the processor from 2-4;

Fig.14 shows the maximum absolute position and orientation errors of the six mobile robots system along iteration axis in simulation and experimental results, where the simulation results for the first 300 iterations and the experimental results for the following 25 iterations. We can see that the max position and orientation errors almost decrease to zero for the first 300 iterations, and have a sudden spike at the 301th iteration as the results come from real robot at this point. Because of the initial state shifts, disturbances and measurements noises in real experimental environment, the experimental error also decreases to a small bound as the same as simulation example in Section IV.A. The output trajectories of the three mobile robots after the $k = 1$, $k = 3$, $k = 10$ and $k = 25$ iterations (the iteration is recount start from real experiment) are shown in Fig.15, It can be observed from Fig.15 that the formation tracking performance is improved as iteration increases.

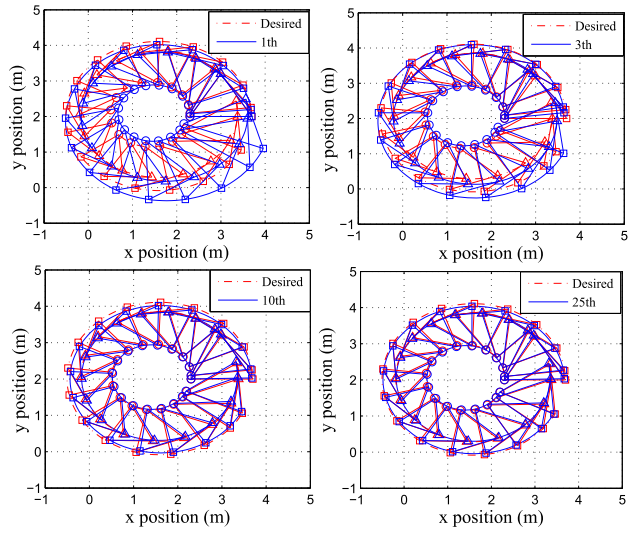

FIGURE 15. Experimental results for tracking performance of robots at 1th, 3th, 10th, 25th.

V. CONCLUSION

In this paper, the robust formation control issue of a group of differential-drive mobile robots in face of the initial state shifts, disturbances, measurement noises and communication

time-delays has been considered. A distribute algorithm is proposed to generate the linear and angular velocity for each mobile robot, which utilizes both the information obtained from previous trial as experience and current formation error to refine the control input. By using the 2-D analysis approach and graph theory, the convergence analysis of the learning processes is addressed. It shows that we can obtain the convergence result of formation error under a matrix norm condition, which provides the guidance on chosen learning gain matrix. The advantage of proposed algorithm compared with the controller only contains the predictive learning term and the controller ignores the affect of time delay is illustrated by simulation. The effectiveness of applying the proposed algorithm to real formation task has been demonstrated via the experiment test. The results show that the multi-robot system performs well for formation tracking after multiple repetition. Further study will focus on how to extend the proposed algorithm to solve robust formation control issue of multiple differential-drive mobile robots under switching topology.

APPENDIX A
PROOF OF LEMMA 1

Proof: The proof process is divided into three steps by using the inductive analysis approach:

Step 1: Let $t = 0$, and we prove that $\limsup_{k\to\infty} \|\Delta\xi_k(1)\| \le b_7(1)$, $\limsup_{k\to\infty} \|\Delta\eta_k(1)\| \le b_8(1)$ and $\limsup_{k\to\infty} \|\Delta u_k(1)\| \le b_9(1)$, where $b_7(1) \ge 0$, $b_8(1) \ge 0$ and $b_9(1) \ge 0$ are a certain bound depending on b_1, b_2, b_3, b_4 and/or b_5.

According inequation (19), we can direct obtain that:

$$\begin{aligned}\limsup_{k\to\infty} \|\Delta\xi_k(1)\| &\le \theta_{11}b_4 + \theta_{12}b_5 + \theta_{13}\times 0 + \theta_{14}b_6 + b_1\\ &\le b_7(1)\limsup_{k\to\infty} \|\Delta\eta_k(1)\|\\ &\le \theta_{21}b_4 + \theta_{22}b_5 + \theta_{23}\times 0 + \theta_{24}b_6 + b_2\\ &\le b_8(1)\end{aligned}$$

and

$$\begin{aligned}\|\Delta u_{k+1}(1)\| &\le [\theta_{31}b_7(1) + \theta_{32}b_8(1) + \theta_{33}\times 0 + b_3] + \theta_{34}\|\Delta u_k(1)\|\\ &\le [\theta_{31}b_7(1) + \theta_{32}b_8(1) + b_3]\sum_{i=0}^{k}\theta_{34}^i + \theta_{34}^{k+1}\|\Delta u_0(1)\|\end{aligned}$$

By noting the condition that $0 \le \theta_{34} < 1$ and $\|\Delta u_0(0)\| \le b_6$, we can obtain

$$\begin{aligned}\limsup_{k\to\infty} \|\Delta u_{k+1}(1)\| &\le [\theta_{31}b_7(1) + \theta_{32}b_8(1) + b_3](1-\theta_{34})^{-1}\\ &\le b_9(1)\end{aligned}$$

where $b_7(1)$, $b_8(1)$, $b_9(1)$ are denote as

$$\begin{aligned}b_7(1) &= \theta_{11}b_4 + \theta_{12}b_5 + \theta_{14}b_6 + b_1\\ b_8(1) &= \theta_{21}b_4 + \theta_{22}b_5 + \theta_{24}b_6 + b_2\\ b_9(1) &= [\theta_{31}b_7(1) + \theta_{32}b_8(1) + b_3](1-\theta_{34})^{-1}\end{aligned}$$

Step 2: Given any time step $t \ge 0$, we assume that for all time steps $l = 0, 1, \ldots, t$, we have $\limsup_{k\to\infty} \|\Delta\xi_k(l)\| \le b_7(l)$, $\limsup_{k\to\infty} \|\Delta\eta_k(l)\| \le b_8(l)$ and $\limsup_{k\to\infty} \|\Delta u_k(l)\| \le b_9(l)$ hold where $b_7(l) \ge 0$, $b_8(l) \ge 0$ and $b_9(l) \ge 0$ are certain bounded depending on b_1, b_2, b_3, b_4 and/or b_5. Then we will prove that we can find $b_7(t+1) \ge 0$, $b_8(t+1) \ge 0$ and $b_9(t+1) \ge 0$ to guarantee $\limsup_{k\to\infty} \|\Delta\xi_k(t+1)\| \le b_7(t+1)$, $\limsup_{k\to\infty} \|\Delta\eta_k(t+1)\| \le b_8(t+1)$ and $\limsup_{k\to\infty} \|\Delta u_k(t+1)\| \le b_9(t+1)$, where $b_7(t+1) \ge 0$, $b_8(t+1) \ge 0$ and $b_9(t+1) \ge 0$ are certain bounded depending on b_1, b_2, b_3, b_4 and/or b_5.

At first, take the limit of $k \to \infty$ at both sides of the inequations at the first two lines of (19), we deduce that:

$$\begin{aligned}\limsup_{k\to\infty} \|\Delta\xi_k(t+1)\| &\le \theta_{11}\limsup_{k\to\infty} \|\Delta\xi_k(t)\| + \theta_{12}\limsup_{k\to\infty} \|\Delta\eta_k(t)\|\\ &\quad + \theta_{13}\sum_{d=0}^{\min(\tau_{\max},t)}\limsup_{k\to\infty} \|\Delta\eta_k(t-d)\|\\ &\quad + \theta_{14}\limsup_{k\to\infty} \|\Delta u_k(t)\| + b_1\\ &\le \theta_{11}b_7(t) + \theta_{12}b_8(t) + \theta_{13}\sum_{d=0}^{\min(\tau_{\max},t)} b_8(t-d)\\ &\quad + \theta_{14}b_9(t) + b_1\\ &\le b_7(t+1)\end{aligned}$$

$$\begin{aligned}\limsup_{k\to\infty} \|\Delta\eta_k(t+1)\| &\le \theta_{21}\limsup_{k\to\infty} \|\Delta\xi_k(t)\| + \theta_{22}\limsup_{k\to\infty} \|\Delta\eta_k(t)\|\\ &\quad + \theta_{23}\sum_{d=0}^{\min(\tau_{\max},t)}\limsup_{k\to\infty} \|\Delta\eta_k(t-d)\|\\ &\quad + \theta_{24}\limsup_{k\to\infty} \|\Delta u_k(t)\| + b_1\\ &\le \theta_{21}b_7(t) + \theta_{22}b_8(t) + \theta_{23}\sum_{d=0}^{\min(\tau_{\max},t)} b_8(t-d)\\ &\quad + \theta_{24}b_9(t) + b_2\\ &\le b_8(t+1)\end{aligned}$$

Then consider the time $t+1$ and $k+1$th iteration for the third line of (19), we have:

$$\begin{aligned}&\|\Delta u_{k+1}(t+1)\|\\ &\le \Big[\theta_{31}\|\Delta\xi_k(t+1)\| + \theta_{32}\|\Delta\eta_k(t+1)\| + \theta_{33}\sum_{d=0}^{\min(\tau_{\max},t)}\|\Delta\eta_k(t-d)\| + b_3\Big]\\ &\quad + \theta_{34}\|\Delta u_k(t+1)\|\end{aligned}$$

$$\leq \Big[\theta_{31}\|\Delta\xi_k(t+1)\| + \theta_{32}\|\Delta\eta_k(t+1)\| + \theta_{33}\sum_{d=0}^{\min(\tau_{\max},t)}\|\Delta\eta_k(t-d)\| + b_3\Big]\sum_{i=0}^{k}\theta_{34}^{i} + \theta_{34}^{k+1}\|\Delta u_0(t+1)\|$$

Take the limit of $k \to \infty$ at both sides of the inequality above, and combine with the condition that $0 \leq \theta_{33} < 1$, we can deduce that:

$$\begin{aligned}&\limsup_{k\to\infty}\|\Delta u_{k+1}(t+1)\| \\ &\leq \Big[\theta_{31}b_7(t+1) + \theta_{32}b_8(t+1) + \theta_{33}\sum_{d=0}^{\min(\tau_{\max},t)} b_8(t-d) + b_3\Big](1-\theta_{34})^{-1} \\ &\leq b_9(t+1)\end{aligned}$$

where $b_7(t+1)$, $b_8(t+1)$, $b_9(t+1)$ are denoted as

$$\begin{aligned}b_7(t+1) &= \theta_{11}b_7(t) + \theta_{12}b_8(t) + \theta_{13}\sum_{d=0}^{\min(\tau_{\max},t)} b_8(t-d) + \theta_{14}b_9(t) + b_1 \\ b_8(t+1) &= \theta_{21}b_7(t) + \theta_{22}b_8(t) + \theta_{23}\sum_{d=0}^{\min(\tau_{\max},t)} b_8(t-d) + \theta_{24}b_9(t) + b_2 \\ b_9(t+1) &= \Big[\theta_{31}b_7(t+1) + \theta_{32}b_8(t+1) + \theta_{33}\sum_{d=0}^{\min(\tau_{\max},t)} b_8(t-d) + b_3\Big](1-\theta_{34})^{-1}\end{aligned}$$

Step 3: Let $b_7 = max_{t\in[1,T]}b_7(t)$, $b_8 = max_{t\in[1,T]}b_8(t)$ and $b_9 = max_{t\in[1,T]}b_9(t)$, Based on the previous two steps, we can gain that $\limsup_{k\to\infty}\|\Delta\xi_k(t)\| \leq b_7$, $\limsup_{k\to\infty}\|\Delta\eta_k(t)\| \leq b_8$ and $\limsup_{k\to\infty}\|\Delta u_k(t)\| \leq b_9$. Thus this lemma can be proofed completely. ■

REFERENCES

[1] W. Guanghua, L. Deyi, G. Wenyan, and J. Peng, "Study on formation control of multi-robot systems," in *Proc. Int. Conf. Intell. Syst. Design Eng. Appl.*, 2013, pp. 1335–1339.
[2] F. Yan, B. Li, W. Shi, and D. Wang, "Hybrid visual servo trajectory tracking of wheeled mobile robots," *IEEE Access*, vol. 6, pp. 24291–24298, 2018.
[3] F. A. X. Da Mota, M. X. Rocha, J. J. P. C. Rodrigues, V. H. C. De Albuquerque, and A. R. De Alexandria, "Localization and navigation for autonomous mobile robots using Petri nets in indoor environments," *IEEE Access*, vol. 6, pp. 31665–31676, 2018.
[4] Y. Zhang and L. E. Parker, "IQ-ASyMTRe: Forming executable coalitions for tightly coupled multirobot tasks," *IEEE Trans. Robot.*, vol. 29, no. 2, pp. 400–416, Apr. 2013.
[5] T. Suzuki, T. Sekine, T. Fujii, H. Asama, and I. Endo, "Cooperative formation among multiple mobile robot teleoperation in inspection task," in *Proc. IEEE Conf. Decis. Control*, vol. 1, Dec. 2000, pp. 358–363.
[6] R. Vidal, O. Shakernia, H. J. Kim, D. H. Shim, and S. Sastry, "Probabilistic pursuit-evasion games: Theory, implementation, and experimental evaluation," *IEEE Trans. Robot. Autom.*, vol. 18, no. 5, pp. 662–669, Oct. 2002.
[7] J. Shao, G. Xie, and L. Wang, "Leader-following formation control of multiple mobile vehicles," *IET Control Theory Appl.*, vol. 1, no. 2, pp. 545–552, Mar. 2007.
[8] G. Antonelli, E. Arrichiello, and S. Chiaverini, "Experiments of formation control with multirobot systems using the null-space-based behavioral control," *IEEE Trans. Control Syst. Technol.*, vol. 17, no. 5, pp. 1173–1182, Sep. 2009.
[9] Y. Jia, "Robust control with decoupling performance for steering and traction of 4WS vehicles under velocity-varying motion," *IEEE Trans. Control Syst. Technol.*, vol. 8, no. 3, pp. 554–569, May 2000.
[10] L. Peng, F. Guan, L. Perneel, H. Fayyad-Kazan, and M. Timmerman, "Decentralized multi-robot formation control with communication delay and asynchronous clock," *J. Intell. Robot. Syet.*, vol. 89, nos. 3–4, pp. 465–484, 2018.
[11] R. Olfati-Saber and R. M. Murray, "Consensus problems in networks of agents with switching topology and time-delays," *IEEE Trans. Autom. Control*, vol. 49, no. 9, pp. 1520–1533, Sep. 2004.
[12] B. Ranjbar-Sahraei, F. Shabaninia, A. Nemati, and S. Stan, "A novel robust decentralized adaptive fuzzy control for swarm formation of multiagent systems," *IEEE Trans. Ind. Electron.*, vol. 59, no. 8, pp. 3124–3134, Aug. 2012.
[13] M. Jahangir, S. Khosravi, and H. Afkhami, "A robust-adaptive fuzzy coverage control for robotic swarms," *Nonlinear Dyn.*, vol. 69, no. 3, pp. 1191–1201, 2012.
[14] W. Dong, "Robust formation control of multiple wheeled mobile robots," *J. Intell. Robot. Syst.*, vol. 62, nos. 3–4, pp. 547–565, 2011.
[15] Y. Jia, "Alternative proofs for improved LMI representations for the analysis and the design of continuous-time systems with polytopic type uncertainty: A predictive approach," *IEEE Trans. Autom. Control*, vol. 48, no. 8, pp. 1413–1416, Aug. 2003.
[16] M. Franceschelli, A. Pisano, A. Giua, and E. Usai, "Finite-time consensus with disturbance rejection by discontinuous local interactions in directed graphs," *IEEE Trans. Autom. Control*, vol. 60, no. 4, pp. 1133–1138, Apr. 2015.
[17] P. He, Y. Li, and J. H. Park, "Noise tolerance leader-following of high-order nonlinear dynamical multi-agent systems with switching topology and communication delay," *J. Franklin Inst.*, vol. 353, no. 1, pp. 108–143, 2016.
[18] Y. Jia, "General solution to diagonal model matching control of multiple-output-delay systems and its applications in adaptive scheme," *Prog. Natural Sci.*, vol. 19, no. 1, pp. 79–90, 2009.
[19] J. Lai, S. Chen, X. Lu, and H. Zhou, "Formation tracking for nonlinear multi-agent systems with delays and noise disturbance," *Asian J. Control*, vol. 17, no. 3, pp. 879–891, 2015.
[20] Y. Liu and Y. Jia, "H_∞ consensus control of multi-agent systems with switching topology: A dynamic output feedback protocol," *Int. J. Control*, vol. 83, no. 3, pp. 527–537, 2010.
[21] S. Arimoto, S. Kawamura, and F. Miyazaki, "Bettering operation of robots by learning," *J. Robot. Syst.*, vol. 1, no. 2, pp. 123–140, 1984.
[22] D. A. Bristow, M. Tharayil, and A. G. Alleyne, "A survey of iterative learning control," *IEEE Control Syst. Mag.*, vol. 26, no. 3, pp. 96–114, Jun. 2006.
[23] H.-S. Ahn, Y. Q. Chen, and K. L. Moore, "Iterative learning control: Brief survey and categorization," *IEEE Trans. Syst., Man, Cybern. C, Appl. Rev.*, vol. 37, no. 6, pp. 1099–1121, Nov. 2007.
[24] J.-X. Xu, "A survey on iterative learning control for nonlinear systems," *Int. J. Control*, vol. 84, no. 7, pp. 1275–1294, Jul. 2011.
[25] A. Rezaeizadeh and R. S. Smith, "Iterative learning control for the radio frequency subsystems of a free-electron laser," *IEEE Trans. Control Syst. Technol.*, vol. 26, no. 5, pp. 1567–1577, Sep. 2018.
[26] Q. Yu, Z. Hou, and J.-X. Xu, "D-type ILC based dynamic modeling and norm optimal ILC for high-speed trains," *IEEE Trans. Control Syst. Technol.*, vol. 26, no. 2, pp. 652–663, Mar. 2018.
[27] J. Liu, X. Dong, D. Huang, and M. Yu, "Composite energy function-based spatial iterative learning control in motion systems," *IEEE Trans. Control Syst. Technol.*, vol. 26, no. 5, pp. 1834–1841, Sep. 2018.
[28] C. T. Freeman, "Upper limb electrical stimulation using input-output linearization and iterative learning control," *IEEE Trans. Control Syst. Technol.*, vol. 23, no. 4, pp. 1546–1554, Jul. 2015.
[29] J. X. Xu, D. Huang, V. Venkataramanan, and T. C. T. Huynh, "Extreme precise motion tracking of piezoelectric positioning stage using sampled-data iterative learning control," *IEEE Trans. Control Syst. Technol.*, vol. 21, no. 4, pp. 1432–1439, Jul. 2013.
[30] H.-S. Ahn and Y. Chen, "Iterative learning control for multi-agent formation," in *Proc. ICROS-SICE Int. Joint Conf.*, 2009, pp. 3111–3116.
[31] Y. Liu and Y. Jia, "An iterative learning approach to formation control of multi-agent systems," *Syst. Control Lett.*, vol. 61, no. 1, pp. 148–154, 2012.

[32] D. Meng, Y. Jia, and J. Du, "Robust consensus tracking control for multiagent systems with initial state shifts, disturbances, and switching topologies," *IEEE Trans. Neural Netw. Learn. Syst.*, vol. 26, no. 4, pp. 809–824, Apr. 2015.
[33] L. Sheng, Y.-J. Pan, and X. Gong, "Consensus formation control for a class of networked multiple mobile robot systems," *J. Control Sci. Eng.*, vol. 2012, no. 9, 2012, Art. no. 150250.
[34] W. Ren, "Consensus tracking under directed interaction topologies: Algorithms and experiments," *IEEE Trans. Control Syst. Technol.*, vol. 18, no. 1, pp. 230–237, Jan. 2010.
[35] J.-X. Xu, S. Zhang, and S. Yang, "A HOIM-based iterative learning control scheme for multi-agent formation," in *Proc. IEEE Int. Symp. Intell. Control*, Sep. 2011, pp. 418–423.
[36] C. Yu and X. Chen, "Trajectory tracking of wheeled mobile robot by adopting iterative learning control with predictive, current, and past learning items," *Robotica*, vol. 33, no. 7, pp. 1393–1414, 2015.
[37] M. K. Kang, J. S. Lee, and K. L. Han, "Kinematic path-tracking of mobile robot using iterative learning control," *J. Robot. Syst.*, vol. 22, no. 2, pp. 111–121, 2005.
[38] D. Meng and K. L. Moore, "Robust cooperative learning control for directed networks with nonlinear dynamics," *Automatica*, vol. 75, pp. 172–181, Jan. 2017.
[39] D. C. Mazur, R. D. Quint, and V. A. Centeno, "Time synchronization of automation controllers for power applications," *IEEE Trans. Ind. Appl.*, vol. 50, no. 1, pp. 25–32, Jan. 2014.
[40] W. Ren and R. W. Beard, "Consensus seeking in multiagent systems under dynamically changing interaction topologies," *IEEE Trans. Autom. Control*, vol. 50, no. 5, pp. 655–661, May 2005.

SHIHAO SUN received the Ph.D. degree in applied mathematics from Beihang University, Beijing, China, in 2018. His current research interests include iterative learning control and distributed control of multiagent systems.

TAKAHIRO ENDO received the Ph.D. (Dr. Eng.) degree from the Tokyo Institute of Technology, Japan, in 2006. Since 2015, he has been with the Department of Mechanical Engineering and Science, Kyoto University, Kyoto, Japan, where he is currently an Assistant Professor. His research interests include haptic interfaces, robotics, and the control of infinite dimensional systems.

FUMITOSHI MATSUNO received the Ph.D. (Dr. Eng.) degree from Osaka University, Toyonaka, Japan, in 1986. In 1986, he joined the Department of Control Engineering, Osaka University. Since 2009, he has been a Professor with the Department of Mechanical Engineering and Science, Kyoto University, Kyoto, Japan. He is also the Vice President with the Institute of Systems, Control and Information Engineers, Kyoto, and the NPO International Rescue System Institute, Kobe, Japan. His current research interests include robotics, swarm intelligence, control of distributed parameter system and nonlinear system, and rescue support system in disaster.

Dr. Matsuno is a Fellow Member of the SICE, the JSME, and the Robotics Society of Japan. He was a recipient of many awards, including the Outstanding Paper Award in 2001 and 2006, respectively, the Takeda Memorial Prize in 2001 from the Society of Instrument and Control Engineers (SICE), the Prize for Academic Achievement from the Japan Society of Mechanical Engineers (JSME) in 2009, and the Best Paper Award in 2013 from the Information Processing Society of Japan.